論文 / 著書情報
Article / Book Information

Title	A Biologically Inspired Biped Locomotion Strategy for Humanoid Robots: Modulation of Sinusoidal Patterns by a Coupled Oscillator Model
Author	Jun Morimoto, Gen Endo, Jun Nakanish, Gordon Cheng
Journal/Book name	IEEE Transaction on Robotics, Vol. 24, No. 1, pp. 185-191
Issue date	2008, 1
DOI	http://dx.doi.org/10.1109/TRO.2008.915457
URL	http://www.ieee.org/index.html
Copyright	(c)2008 IEEE. Personal use of this material is permitted. Permission from IEEE must be obtained for all other users, including reprinting/republishing this material for advertising or promotional purposes, creating new collective works for resale or redistribution to servers or lists, or reuse of any copyrighted components of this work in other works.
Note	このファイルは著者（最終）版です。 This file is author (final) version.

A Biologically Inspired Biped Locomotion Strategy for Humanoid Robots: Modulation of Sinusoidal Patterns by a Coupled Oscillator Model

Jun Morimoto (corresponding author), Gen Endo, Jun Nakanishi, *Member, IEEE*, and Gordon Cheng, *Senior Member, IEEE*

***Abstract*—Biological systems seem to have a simpler but more robust locomotion strategy than existing biped walking controllers for humanoid robots. We show that a humanoid robot can step and walk using simple sinusoidal desired joint trajectories with their phase adjusted by a coupled oscillator model. We use the center of pressure location and velocity to detect the phase of the lateral robot dynamics. This phase information is used to modulate the desired joint trajectories. We do not explicitly use dynamical parameters of the humanoid robot. We hypothesize that a similar mechanism may exist in biological systems. We applied the proposed biologically inspired control strategy to our newly developed human-sized humanoid robot CB and a small size humanoid robot, enabling them to generate successful stepping and walking patterns.**

***Index Terms*—Biped Walking, Humanoid Robots, Central Pattern Generator, Coupled Oscillator, Biologically Inspired Approach**

I. INTRODUCTION

BIOLOGICAL systems seem to have a simpler but more robust locomotion strategy [1] than existing biped walking controllers for humanoid robots (e.g. [2]). For examples, [2] and [3] showed that the cat locomotion system can generate walking pattern without using higher brain function. An early study of biologically inspired approach to bipedal locomotion [4] suggested that synchronization property of neural system with periodic sensor inputs plays an important role for robust locomotion control. After this leading study, there is growing interest in biologically inspired locomotion control utilizing coupled neural oscillators [5]–[8] or using a phase oscillator model with phase reset methods [9], [10]. These studies make use of foot contact information, or ground reaction forces in exploiting the entrainment property of the neural or phase oscillator model.

J. Morimoto is with the Japan Science and Technology, 4-1-8 Honcho, Kawaguchi, Saitama, 332-0012, Japan, and with ATR computational neuroscience labs, 2-2-2 Hikari-dai, Seika-cho, Souraku-gun, Kyoto, 619-0288, Japan (e-mail: xmorimo@atr.jp)

G. Endo is with Dept. of Mechanical and Aerospace Engineering, Tokyo Institute of Technology, 4-1-8 Honcho, Kawaguchi, Saitama, 332-0012, Japan. (e-mail: gendo@sms.titech.ac.jp)

J. Nakanishi is with the Japan Science and Technology, 4-1-8 Honcho, Kawaguchi, Saitama, 332-0012, Japan, and with ATR computational neuroscience labs, 2-2-2 Hikari-dai, Seika-cho, Souraku-gun, Kyoto, 619-0288, Japan (e-mail: jun@atr.jp)

G. Cheng is with the Japan Science and Technology, 4-1-8 Honcho, Kawaguchi, Saitama, 332-0012, Japan, and with ATR computational neuroscience labs, 2-2-2 Hikari-dai, Seika-cho, Souraku-gun, Kyoto, 619-0288, Japan (e-mail: gordon@atr.jp)

Similarly, since biped walking is a periodic movement, it has been suggested that methods to synchronize biped controllers with the robot dynamics are useful to generate stable walking patterns. Several studies designed walking trajectories as a function of a physical variable of the robot (e.g. ankle joint angle) [11]–[13].

However, a neural oscillator model has complex dynamics and many parameters to be selected [4], [5]. Other approaches that has synchronization mechanisms usually require proper gait design [9], [10], [12], [13].

In this study, we undertake the development of a simple but robust biped controller by means of a coupled oscillator system, which is said to exist in vertebrates and is widely referred as central pattern generator (CPG) [14].

Many biped walking studies have emphasized that humanoid robots have inverted pendulum dynamics, with the top at the center of mass and the base at the center of pressure, and proposed control strategies to stabilize the dynamics [15]–[19].

We propose using the center of pressure to detect the phase of the inverted pendulum dynamics. 1) We use simple periodic functions (sinusoids) as desired joint trajectories. 2) We show that synchronization of the desired trajectories at each joint with the inverted pendulum dynamics can generate stepping and walking. 3) Since our nominal gait patterns are sinusoids, our approach does not need careful design of desired gait trajectories. 4) We use smaller numbers of parameters than existing neural oscillator approach, and compare to the neural oscillator model, parameters used in our approach can be easily selected since the physical meanings of the parameters are quite simple.

To the best of our knowledge, this study is the first attempt to apply an oscillator model to a human-sized humanoid robot CB [20] (Fig.1(a)) for biped walking in a real environment. We also apply our method to a small humanoid robot (Fig.1(b)). First, we introduce our biologically inspired biped locomotion strategy, which use modulated sinusoidal patterns via a coupled oscillator model, described in Section II. In Section III, we apply our proposed approach to the simulated robot model (see Fig. 1(c)), and also show our experimental results.

II. MODULATION OF SINUSOIDAL PATTERNS BY A COUPLED OSCILLATOR MODEL

Our biped control approach uses a coupled phase oscillator model [21] to modulate sinusoidal patterns. The aim of using

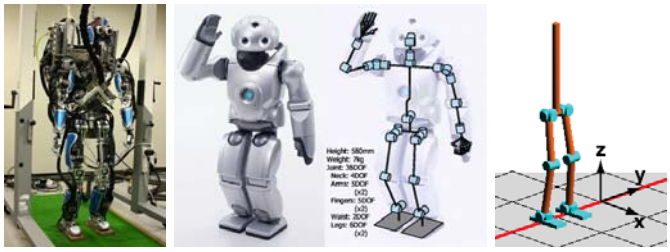

(a) (b) (c)

Fig. 1. (a) Our human-sized hydraulic humanoid robot CB developed by SARCOS [20]. height: 1.59 m, total weight: 95 kg. (b) Small humanoid robot used in the experiment. (c) Simple 3D biped simulation model. The biped model has ten degrees of freedom. height: 1.59 m, total weight: 95 kg.

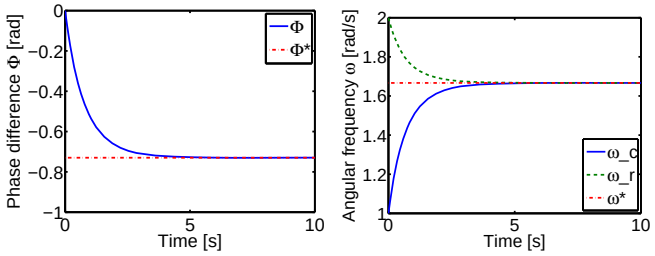

(a) Phase difference (b) Angular frequency

Fig. 2. Typical time profile of the coupled oscillator system. (a) Phase difference $\Psi = \phi_r - \phi_c$. The phase difference converged to the analytically derived value Ψ^* depicted by dash dot line. (b) Angular frequencies ω_r and ω_c. Angular frequency of each oscillator converged to the analytically derived compromise frequency ω^*.

the coupled phase oscillator model is to synchronize periodic patterns generated by the controller with the dynamics of the robot.

We also show a strategy to design nominal desired joint angle. One of the simplest way to generate periodic pattern at each joint is using only one sinusoidal basis function to represent the desired joint angle. By only using one sinusoidal basis function at each joint, we have smallest numbers of parameters to represent periodic patterns at each joint. We introduce our stepping and walking controllers that use the desired joint angle represented by the sinusoidal function.

A. Coupled oscillator model

Here, we consider the behavior of the following dynamics of the phase of a biped controller ϕ_c and the phase of the robot dynamics ϕ_r:

$$\dot{\phi}_c = \omega_c + K_c \sin(\phi_r - \phi_c), \quad (1)$$

$$\dot{\phi}_r = \omega_r + K_r \sin(\phi_c - \phi_r), \quad (2)$$

where $\omega_c > 0$ and $\omega_r > 0$ are natural frequencies of the controller and the robot dynamics, and K_c, K_r are positive coupling constants. We can find two fixed points if $|\omega_c - \omega_r| < K_c + K_r$. There is no fixed point if $|\omega_c - \omega_r| > K_c + K_r$. A saddle-node bifurcation occurs when $|\omega_c - \omega_r| = K_c + K_r$.

If $|\omega_c - \omega_r| < K_c + K_r$, the oscillators run with the phase difference: $\Psi^* = \phi_r - \phi_c = \sin^{-1}((\omega_r - \omega_c)/(K_c + K_r))$ and the compromise frequency: $\omega^* = (K_r\omega_c + K_c\omega_r)/(K_c + K_r)$ when they are entrained [21].

We showed the typical time profile of phase difference $\Phi = \phi_c - \phi_r$, angular frequencies ω_c and ω_r in Fig. 2. Although usually the biped dynamics can not represented by the simple phase dynamics (2), we can still detect the phase from the robot dynamics as described in Section II-B. Then, we use (1) to adjust phase of the controller under assumption that the phase dynamics detected from the biped dynamics keeps similar property to (2).

B. Phase detection from the robot dynamics

As previous studies have pointed out, controlling the inverted pendulum dynamics represented by the center of mass and the center of pressure (Fig. 3(a)) is a major issue in controlling biped robots. We consider the inverted pendulum dynamics on lateral plane that has a four dimensional state space $\mathbf{x} = (y, \dot{y}, \psi^r, \dot{\psi}^r)$, which depicted in Fig. 3(a).

To detect phase from the inverted pendulum dynamics, we project the four-dimensional state space to a two-dimensional state space. Then, convert the two-dimensional state space to the phase space by using the function $\arctan$, which widely used as phase detector for radio wave decoding.

In this study, we consider the center of pressure y and the velocity of the center of pressure $\dot{y}$ as the variables in the two-dimensional state space since detecting these values by force sensors on soles is easy for our real robots. Therefore, we detect the phase as

$$\phi_r(\mathbf{x}) = -\arctan\left(\frac{\dot{y}}{y}\right). \quad (3)$$

C. Simplified COP detection

The center of pressure (COP) depends on a coordinate system, and we need a kinematic model to detect COP. Alternatively, we use an approximate center of pressure:

$$y = \frac{y^l_{foot} F^l_z + y^r_{foot} F^r_z}{F^r_z + F^l_z}, \quad (4)$$

where F^l_z and F^r_z represent the left and right ground reaction force respectively, and y^l_{foot} and y^r_{foot} are the lateral position of each foot. We assume that feet are symmetrically placed $-y^l_{foot} = y^r_{foot}$. Because we only use this center of pressure to detect the phase of the robot dynamics $\phi_r(\mathbf{x})$ in equation (3), the scale of the foot position y^l_{foot} and y^r_{foot} can be arbitrary. We simply set $y^l_{foot} = -y^r_{foot} = 1.0$ m. This simplified COP detection does not require the kinematic model.

When we derive the center of pressure from the sensor input, we use a low-pass filter to eliminate sensor noise from force sensors on soles.

Note that when the center of pressure come to an edge of a sole, the detected $\phi_r(\mathbf{x})$ may have discontinuous change because of discontinuous change of the velocity of the center of pressure (see (3)). However, because we apply the low-pass filter to the force sensor input, the filtered velocity of the center of pressure do not have such undesirable discontinuous change.

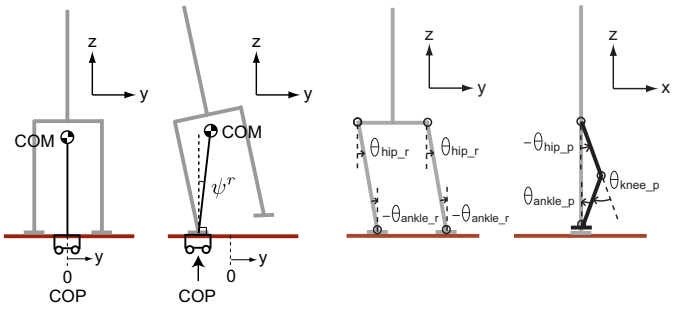

Fig. 3. (a) Inverted pendulum model represented by the center of pressure (COP) and the center of mass (COM). (b) Stepping controller.

D. Phase coordination

In this study, we use two oscillators with phases ϕ_{c_i}, where $i = 1, 2$. We introduce coupling between the oscillators and the phase of the robot dynamics $\phi_r(\mathbf{x})$ to regulate the desired phase relationship between the oscillators as in (1):

$$\dot{\phi}_{c\_i} = \omega_c + K_c \sin((\phi_r(\mathbf{x}) - \alpha_i) - \phi_{c\_i}), \tag{5}$$

where α_i is the desired phase difference. We use two different phase differences, $\{\alpha_1, \alpha_2\} = \{-1/2\pi, 1/2\pi\}$, to make symmetric patterns for a stepping movement by left and right limbs (see section II-E2). Two parameters $\{\omega_c, K_c\}$ need to be selected to define the phase oscillator dynamics.

We empirically found that the natural frequency of a linear pendulum with the length l can be a good candidate for the natural frequency of the controller as $\omega_c = \sqrt{g/l}$, where g denotes the acceleration due to the gravity and l denotes the height of COM when a biped stand straight.

By considering the insight from the oscillator dynamics (1) and (2), we need to use sufficiently large coupling constant K_c to satisfy $|\omega_c - \omega_r| < K_c + K_r$ for keeping fixed points.

E. Stepping controller for lateral movement

1) Side-to-side controller for lateral movement: First, we introduce a controller to generate side-to-side movement. We use the hip joints θ_{hip_r} and the ankle joints θ_{ankle_r} (Fig. 3(b)) for the movement. Desired joint angles for each joint are:

$$\theta^d_{hip\_r}(\phi_c) = A_r \sin(\phi_c) + \bar{\theta}_r, \tag{6}$$
$$\theta^d_{ankle\_r}(\phi_c) = -A_r \sin(\phi_c) - \bar{\theta}_r, \tag{7}$$

where A_r are the amplitudes of a sinusoidal function for side-to-side movements at the hip and the ankle joints, and we use an oscillator with the phase $\phi_c = \phi_{c\_1}$. $\bar{\theta}_r$ defines the rest posture of the hip, knee, and ankle joints. Two parameters $\{A_r, \bar{\theta}_r\}$ need to be selected for the side-to-side controller.

2) Vertical foot movement to make clearance: To achieve foot clearance, we generate vertical movement of the feet (Fig. 3(b)) by using simple sinusoidal trajectories:

$$\theta^d_{hip\_p}(\phi_c) = A_p \sin(\phi_c) + \bar{\theta}_p, \tag{8}$$
$$\theta^d_{knee\_p}(\phi_c) = -2A_p \sin(\phi_c) - 2\bar{\theta}_p, \tag{9}$$
$$\theta^d_{ankle\_p}(\phi_c) = -A_p \sin(\phi_c) - \bar{\theta}_p, \tag{10}$$

where A_p is the amplitude of a sinusoidal function to achieve foot clearance, $\bar{\theta}_p$ defines the rest posture of the hip, knee, and ankle joints. We use the oscillator with phase $\phi_c = \phi_{c\_1}$ for right limb movement and use the oscillator with phase $\phi_c = \phi_{c\_2}$, which has phase difference $\phi_{c\_2} = \phi_{c\_1} + \pi$, for left limb movement. Two parameters $\{A_p, \bar{\theta}_p\}$ need to be selected for the controller for vertical foot movement.

Because the center of pressure is modulated by the joint angle trajectories, the phase of the controller ϕ_c affects the phase of the robot $\phi_r(\mathbf{x})$ in (3), through the controllers introduced in (6)-(10).

F. Biped walking controller with additional sinusoids

For our biped walking controller, we introduce two additional oscillators $\phi^p_{c\_i}$, where $i = 1, 2$. We then consider phase dynamics:

$$\dot{\phi}^p_{c\_i} = \begin{cases} \omega_c + K^p_c \sin((\phi_r(\mathbf{x}) - \alpha^p_i) - \phi^p_{c\_i}) & \text{(single support)} \\ 0 & \text{(double support)} \end{cases} \tag{11}$$

We set the dynamics of the oscillator $\dot{\phi}^p_{c\_i} = 0$ during double support phase so that we can prevent internal force generated by friction between the ground and the soles, while we keep using the phase dynamics (5) . We use two different phase differences, $\{\alpha^p_1, \alpha^p_2\} = \{0.0, \pi\}$, to make symmetric patterns for a forward movements by left and right limbs. We empirically figured out that we can generate biped walking by setting the coupling constant as $K^p_c = K_c/2$.

To walk forward, the biped need to make forward step. To make forward step at proper timing, we introduce an additional sinusoidal trajectory that has $1/2\pi$ phase difference from the sinusoidal trajectories for the stepping movement:

$$\theta^d_{hip\_s}(\phi^p_c) = A_{h\_s} \sin(\phi^p_c), \tag{12}$$
$$\theta^d_{ankle\_s}(\phi^p_c) = -A_{a\_s} \sin(\phi^p_c), \tag{13}$$

where A_{h_s} and A_{a_s} are amplitudes of sinusoidal functions at the hip and the ankle joints for biped walking. We use the phase $\phi^p_c = \phi^p_{c\_1}$ which has $1/2\pi$ phase difference with ϕ_{c_1}, that is phase of the oscillator for lateral movement, for right limb and use the phase $\phi^p_c = \phi^p_{c\_2}$ which has π phase difference with $\phi^p_{c\_1}$. The desired nominal trajectories for hip and ankle pitch joints in (8) and (10) become:

$$\theta^d_{hip\_p}(\phi_c, \phi^p_c) \leftarrow \theta^d_{hip\_p}(\phi_c) + \theta^d_{hip\_s}(\phi^p_c), \tag{14}$$
$$\theta^d_{ankle\_p}(\phi_c, \phi^p_c) \leftarrow \theta^d_{ankle\_p}(\phi_c) + \theta^d_{ankle\_s}(\phi^p_c). \tag{15}$$

Two parameters $\{A_{h\_s}, A_{a\_s}\}$ need to be selected for the controller for forward movements.

III. SIMULATION AND EXPERIMENTAL RESULT

We applied our proposed method to a simple 3D biped robot model (Fig. 1(c)), our human-sized humanoid robot CB (Fig. 1(a)), and the small humanoid robot (Fig. 1(b)).

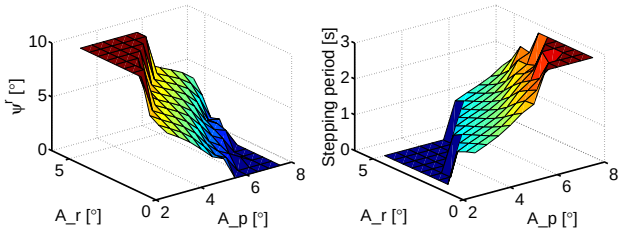

(a) Pendulum angle (b) Stepping period

Fig. 4. Comparison of using different amplitude parameters. (a) Pendulum angle ψ^r in Fig. 3(a). Region has the value $\psi^r = \mathbf{10}$ represents that the robot can not make single support phase with the corresponding parameter selection. Region has the value $\psi^r = \mathbf{0}$ represents that the robot falls over with the corresponding parameter selection. (b) Stepping period. Region has the value $\mathbf{0}$ s represents that the robot can not make single support phase with the corresponding parameter selection. Region has the value $\mathbf{3}$ s represents that the robot falls over with the corresponding parameter selection.

A. Stepping movement

1) Application to the simulated biped model: We applied our proposed method to the biped robot model.

As we proposed in section II-D, the natural frequency of the controller is set as $\omega_c = \sqrt{g/l} = 3.6$ rad/s, and the coupling constant is set as $K_c = 10.0$. Then, we compared different parameter settings for the amplitude A_r in (6), (7) and A_p in (8)-(10).

Figure 4 shows results of the comparison. Using large A_p with small A_r result in falling over. On the other hand, using small A_p with large A_r can not make single support phase. By comparing Fig. 4(a) and 4(b), stepping movement that has smaller pendulum angle ψ^r tends to have larger stepping period.

A proper combination of the parameters $A_r = 2.5°$ and $A_p = 5.0°$, which can make stepping movement without falling over, generated a stepping movement with period 1.4 s. Equivalently, average angular frequency $\dot{\phi}_c^{av} = \frac{1}{T}(\phi_c(T+t) - \phi_c(t))$ of the stepping movement was $\dot{\phi}_c^{av} = 4.5$ rad/s, where T is a stepping period. Figure 5 shows successful stepping of the simulated biped model.

To show how the coupled oscillator model in equation (1) and (2) worked with the biped robot model, we tested a different controller with a different natural frequency, $\omega_c = 2.5$ rad/s. Although the natural frequency was different, the modulated averaged frequency $\dot{\phi}_c^{av} = 3.9$ rad/s was much closer to the previous averaged frequency, $\dot{\phi}_c^{av} = 4.5$ rad/s than the selected natural frequency $\omega_c = 2.5$ rad/s.

By considering the compromise frequency ω^* introduced in section II-A, this result indicates that the current coupling constant $K_c = 10.0$ is large enough to make the controller frequency close to the natural frequency of the robot dynamics.

Figure 6 shows trajectories of desired and actual hip joint angles $\theta^d_{hip\_r}$, θ_{hip_r} (see Fig. 3(b)). Figure 6(a) represents the result of without using a coupled oscillator model. The desired trajectory is the original simple sinusoidal trajectory.

Figure 6(b) represents the result of using a coupled oscillator model. This modulated trajectory made stepping movement possible. Large tracking error appeared during single support phase due to not using very large servo gain. This result shows that our proposed method does not require accurate tracking performance. The desired trajectory is modulated by the coupling with the phase of the robot dynamics $\phi_r(\mathbf{x})$.

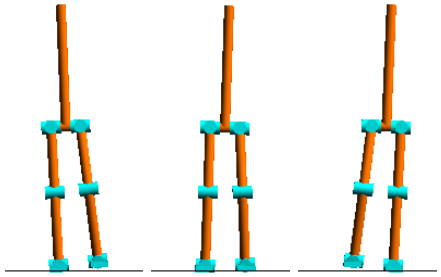

(a) t=0.0 s (b) t=0.4 s (c) t=0.8 s

Fig. 5. Stepping movement using coupled oscillator.

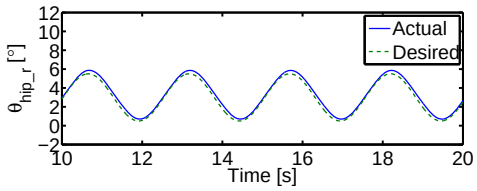

(a) Not using coupled oscillator.

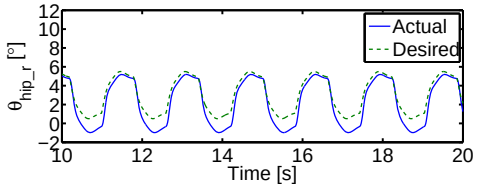

(b) Using coupled oscillator.

Fig. 6. Generated desired and actual trajectory at hip joint. (a) Not using coupled oscillator, (b) Using coupled oscillator. Large tracking error appeared during single support phase due to not using very large servo gain. The result shows that our proposed method does not require accurate tracking performance.

2) Application to human-sized humanoid robot: The proposed stepping method was applied to the human-sized humanoid robot CB.

The natural frequency of the controller is selected as $\omega_c = 3.14$ rad/sec and sufficiently large coupling constant is selected as $K_c = 9.4$ by following the parameter selection approach introduced in Section II-D.

We empirically figured out proper amplitude parameters $A\_r = 3.0°$, and $A_p = 3.5°$, which can generate a stepping movement.

Figure 7 shows successful stepping of the human-sized humanoid robot.

3) Application to the small humanoid robot: We applied the proposed stepping method to the small humanoid robot.

The natural frequency of the controller is selected as $\omega_c = 6.28$ rad/s and sufficiently large coupling constant is selected as $K_c = 9.4$ by following the parameter selection approach introduced in Section II-D.

We empirically figured out proper amplitude parameters $A\_r = 7.5°$ for hip, $A\_r = 2.5°$ for ankle, and $A_p = 3.5°$, which can generate a stepping movement.

Figure 8 shows successful stepping of the small humanoid

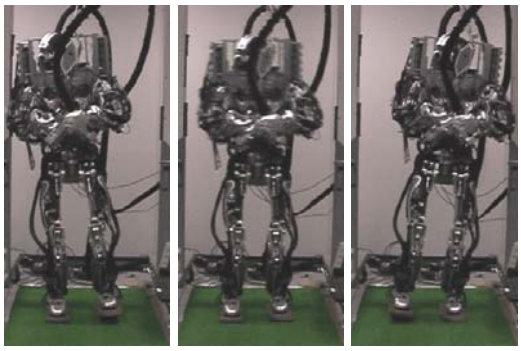

Fig. 7. Successful stepping of our human-sized humanoid robot CB.

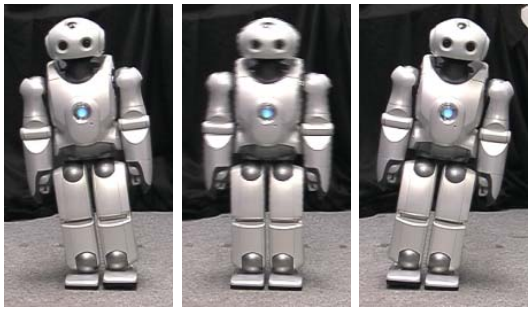

Fig. 8. Successful stepping of the small humanoid robot.

robot.

B. Biped walking

1) Application to simple biped model: We applied our proposed method to generate walking movements by using the simulated biped model.

The same parameters as the stepping controller for the natural frequency of the controller $\omega_c = 3.6$ rad/s, and the coupling constant $K_c = 10.0$ are used. We empirically figured out proper amplitude parameters $A_r = 2.5^\circ$ and $A_p = 6.0^\circ$ for the walking task.

We compared different amplitude parameters A_s by setting $A_{h\_s} = A_s$ in (12) and $A_{a\_s} = A_s/2$ (13).

Figure 9 shows the results of the comparison. Walking velocity was linearly increased according to the increase of the amplitude parameter A_s. This is one of good properties of the proposed walking controller since we can easily select the amplitude parameter to achieve desired walking velocity.

On the other hand, the walking period did not show monotonic change according to the increase of the amplitude A_s as in Fig. 9(b). Walking velocity can be increased by either increase walking step or decrease walking period (increase walking frequency). We can see that walking controller used different strategies to increase walking speed with different amplitude A_s.

Figure 10 shows the successful walking pattern generated by our control approach. We showed that the simulated robot model could walk by only using the simple sinusoidal trajectory, which composed of at most only two sinusoidal basis functions at each joint, modulated by the detected phase from the center of pressure.

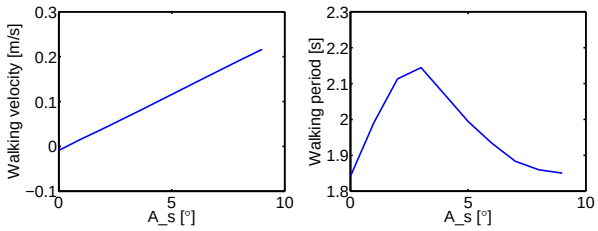

(a) Walking speed (b) Walking period

Fig. 9. Comparison with different amplitude parameters A_s in (12) and (13). The biped model falls over with the parameter $A_s > 9.0^\circ$. (a) Walking speed. (b) Walking period.

2) Application to human-sized humanoid robot: We applied our proposed walking method to the humanoid robot CB.

The same parameters as the stepping controller for the natural frequency of the controller $\omega_c = 3.14$ rad/s, the coupling constant $K_c = 9.4$, $A_r = 3.0^\circ$, and $A_p = 3.5^\circ$ are used.

We empirically figured out proper amplitude parameters $A_{h\_s} = 4.0^\circ$ and $A_{a\_s} = 2.0^\circ$ for the walking task.

Figure 11 shows the successful walking pattern of our humanoid robot. Our proposed method was able to generate successful walking patterns even in the real environment.

Note that the black tube from the top of each photo in figure 11 is a hydraulic cable.

3) Application to the small humanoid robot: We applied our proposed walking method to the small humanoid robot.

The same parameters as the stepping controller for the natural frequency of the controller $\omega_c = 6.28$ rad/s, the coupling constant $K_c = 9.4$, amplitudes $A_{\_r} = 7.5^\circ$ for hip, $A_{\_r} = 2.5^\circ$ for ankle, and $A_p = 3.5^\circ$ are used.

We empirically figured out proper amplitude parameters $A_{h\_s} = 12.0^\circ$ and $A_{a\_s} = 8.0^\circ$ for the walking task.

Figure 12 shows the successful walking pattern of the small humanoid robot. Our proposed method was able to generate successful walking patterns for robots of different sizes. Because our method to design a biped walking controller does not suffered from singularity problem at knee joints that comes from using inverse kinematics, knees can straighten during walking.

We calculated the ratio between the single support phase and double support phase. The ratio was around $(T_{double})/(T_{double} + T_{single}) \times 100\% = 25\%$, where T_{double} is a period of time of double support phase and T_{single} is a period of time of single support phase in a walking cycle. This ratio is similar to the ratio for adult human biped walking $20\% - 25\%$ that depends on the age of the human subject [22], [23]. This ratio is achieved by our proposed controller without using pre-designed trajectories of the center of pressure.

We also tested robustness of our biped controller using four different ground surfaces with different frictions. Each surface also has different height. The four surfaces include carpet with 0.0 mm (base level), plastic sheet with 2.0 mm, rubber sheet with 3.5 mm, and metal sheet with 3.0 mm. Figure 13 shows successful results of walking over the different surfaces without changing any parameter of the biped controller.

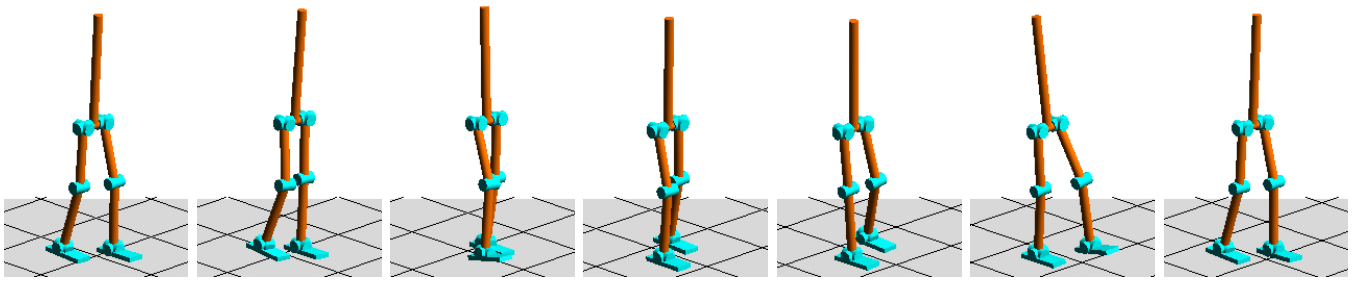

(a) t=0.00 s (b) t=0.30 s (c) t=0.57 s (d) t=0.93 s (e) t=1.23 s (f) t=1.53 s (g) t=1.87 s

Fig. 10. Successful walking pattern using simulated biped robot model. Walking speed is 0.22 m/sec.

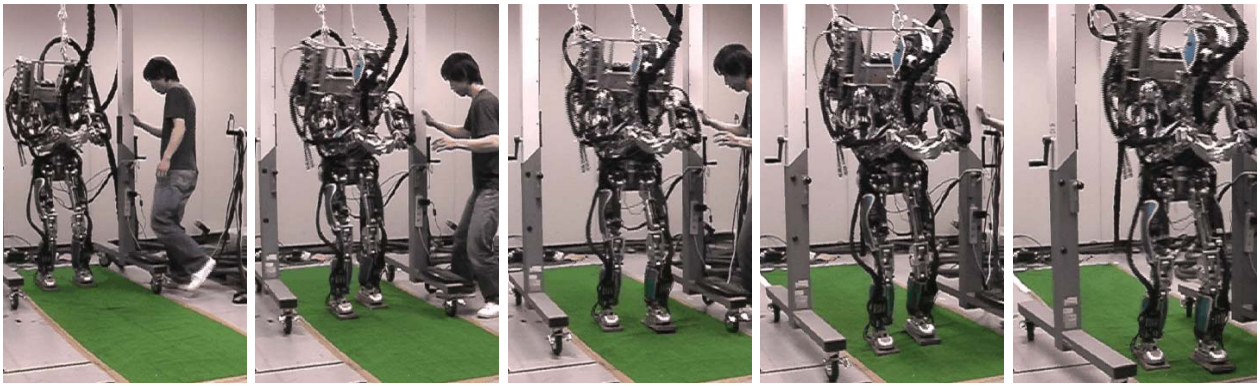

Fig. 11. Successful walking pattern of our human-sized humanoid robot CB.

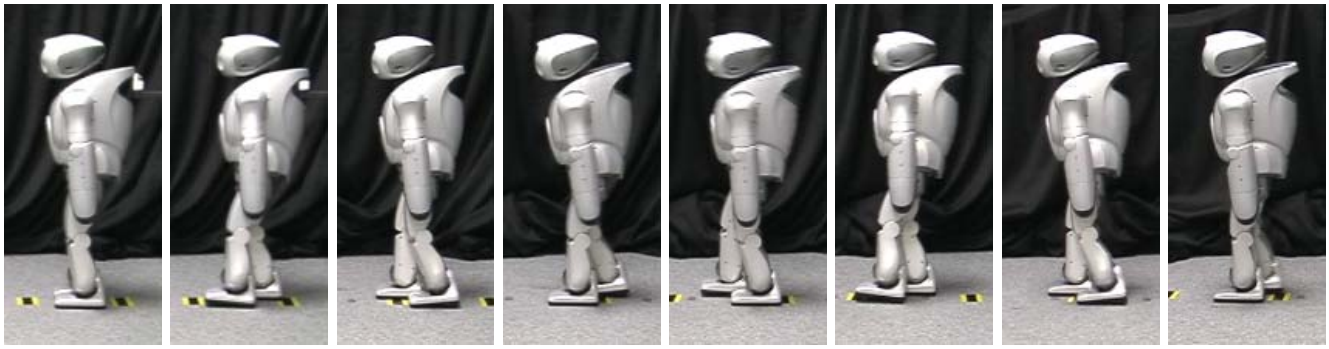

Fig. 12. Successful walking pattern of the small humanoid robot. Knees are stretched during walking.

IV. DISCUSSION

In this paper we presented a biologically inspired biped locomotion strategy. Our method proposed the utilization of the center of pressure position and velocity to detect the phase of the lateral robot dynamics. Evidences in biological locomotion studies support in part of our work [1], [24].

The detected phase of the robot dynamics was used to modulate sinusoidal joint trajectories. The modulated trajectories enabled our robots to generate successful stepping and walking patterns. Because the angular frequency in Equation (5) is continuously changing during stepping and walking, not only the frequency of the controller changes toward the resonant frequency and excites the robot dynamics but also the time course of the sinusoidal patterns are modulated.

We applied successfully our proposed control approach to our newly developed human-sized humanoid robot CB and the small humanoid robot.

In the future, we will consider using optimization methods such as reinforcement learning or dynamic programming [25], [26] to acquire a nonlinear feedback controller in order to increase robustness of the walking controller.

APPENDIX

Here we describe our simulation setups. To follow the desired trajectories, the torque output at each joint is given by a PD servo controller:

$$\boldsymbol{\tau} = \mathbf{K}_p(\boldsymbol{\theta}^d(\phi_c) - \boldsymbol{\theta}) + \mathbf{K}_d(\dot{\boldsymbol{\theta}}^d(\phi_c) - \dot{\boldsymbol{\theta}}), \qquad (16)$$

where $\boldsymbol{\theta}^d(\phi_c) \in \mathbf{R}^{10}$ is the target joint angle vector, $\mathbf{K}_p$ denotes the position gain matrix, and $\mathbf{K}_d$ denotes the velocity gain matrix. Each element of the diagonal position gain matrix $\mathbf{K}_p$ is set to 3000 and each element of the diagonal velocity gain matrix $\mathbf{K}_d$ is set to 100.

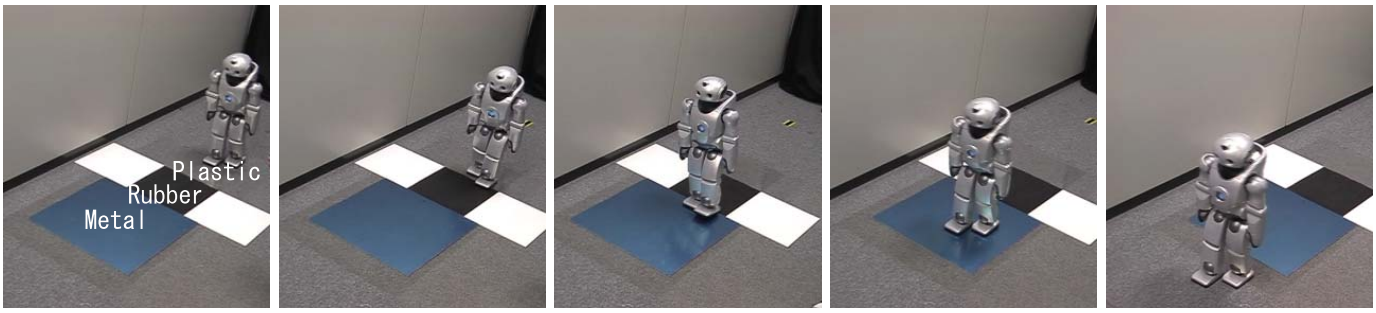

Fig. 13. Successful walking pattern of the small humanoid robot over four different surfaces: (1) Gray carpet, (2) Transparent plastic sheet, (3) Black rubber sheet, (4) Blue metal sheet.

We used the fourth-order Runge-Kutta method with a time step of $\Delta t = 0.0003$ s to numerically integrate the biped dynamics.

The vertical ground reaction force f_z is simulated by a spring-dumper model:

$$f_z = -k_p^z z_{cp} - k_d^z \dot{z}_{cp}, \tag{17}$$

where $k_p^z = 30000$ is the spring gain, $k_d^z = 1000$ is the dumper gain, and z_{cp} denotes vertical position of a contact point.

The ground reaction force for horizontal directions f_x and f_y are simulated by a viscose friction:

$$f_x = -k_d^x \dot{x}_{cp}, \tag{18}$$

$$f_y = -k_d^y \dot{y}_{cp}, \tag{19}$$

where $k_d^x = 2500$ and $k_d^y = 2500$ are dumper gains. x_{cp} and y_{cp} are horizontal position of a contact point.

ACKNOWLEDGMENT

We thank Sony Corp. for allowing us the opportunity to use the small humanoid robot. We thank Darrin Bentivegna for helping us to setup initial experiments. We also thank Mitsuo Kawato, Christopher G. Atkeson, Seiichi Miyakoshi, Sang-Ho Hyon for helpful discussion.

REFERENCES

[1] T. A. McMahon, *Muscles, Reflexes, and Locomotion*. Princeton University Press, 1984.

[2] S. Grillner, "Locomotion in Vertebrates: Central Mechanisms and Reflex Interaction," *Physiol. Review*, vol. 55, pp. 367–371, 1975.

[3] M. L. Shik and G. N. Orlovsky, "Neurophysisology of Locomotion Automatism," *Physiol. Review*, vol. 56, pp. 465–501, 1976.

[4] G. Taga, Y. Yamaguchi, and H. Shimizu, "Self-organized control in bipedal locomotion by neural oscillators in unpredictable environment," *Biological Cybernetics*, vol. 65, pp. 147–159, 1991.

[5] S. Miyakoshi, G. Taga, Y. Kuniyoshi, and A. Nagakubo, "Three dimensional bipedal stepping motion using neural oscillators -towards humanoid motion in the real world," in *IEEE/RSJ Int. Conf. on Intelligent Robots and Systems*, vol. 1, Victoria, Canada, 1998, pp. 84–89.

[6] G. Endo, J. Morimoto, J. Nakanishi, and G. Cheng, "An empirical exploration of a neural oscillator for biped locomotion control," in *Proceedings of IEEE 2004 International Conference on Robotics and Automation*, New Orleans, LA, USA, 2004, pp. 3063–3042.

[7] G. Endo, J. Nakanishi, J. Morimoto, and G. Cheng, "Experimental Studies of a Neural Oscillator for Biped Locomotion with QRIO," in *IEEE Int. Conf. on Robotics and Automation*, Barcelona, Spain, 2005, pp. 598–603.

[8] Y. Fukuoka and H. Kimura, "Adaptive Dynamic Walking of a Quadruped Robot on Irregular Terrain based on Biological Concepts," *Int. Journal of Robotics Research*, vol. 22, no. 2, pp. 187–202, 2003.

[9] K. Tsuchiya, S. Aoi, and K. Tsujita, "Locomotion control of a biped locomotion robot using nonlinear oscillators," in *Proceedings of the IEEE/RSJ International Conference on Intelligent Robots and Systems*, Las Vegas, NV, USA, 2003, pp. 1745–1750.

[10] J. Nakanishi, J. Morimoto, G. Endo, G. Cheng, S. Schaal, and M. Kawato, "Learning from demonstration and adaptation of biped locomotion," *Robotics and Autonomous Systems*, vol. 47, pp. 79–91, 2004.

[11] S. Hyon and T. Emura, "Symmetric Walking Control: Invariance and Global Stability," in *IEEE Int. Conf. on Robotics and Automation*, Barcelona, Spain, 2005, pp. 1456–1462.

[12] M. Doi, Y. Hsegawa, and T. Fukuda, "Passive Trajectory Control of the Lateral Motion in Bipedal Walking," in *IEEE Int. Conf. on Robotics and Automation*, New Orleans, LA, USA, 2004, pp. 3049–3054.

[13] E. R. Westervelt, G. Buche, and J. W. Grizzle, "Experimental validation of a framework for the design ofcontrollers that induce stable walking in planar bipeds," *Int. J. of Robotics Research*, vol. 23, no. 6, pp. 559–582, 2004.

[14] S. Grillner, "Neurobiological bases of rhythmic motor acts in vertebrates," *Science*, vol. 228, pp. 143–149, 1985.

[15] H. Miura and I. Shimoyama, "Dynamical walk of biped locomotion," *Int. J. of Robotics Research*, vol. 3, no. 2, pp. 60–74, 1984.

[16] K. Hirai, M. Hirose, and T. Takenaka, "The Development of Honda Humanoid Robot," in *Proceedings of the 1998 IEEE International Conference on Robotics and Automation*, 1998, pp. 160–165.

[17] K. Nagasaka, M. Inaba, and H. Inoue, "Stabilization of dynamic walk on a humanoid using torso position compliance control," in *Proceedings of 17th Annual Conference on Robotics Society of Japan*, 1999, pp. 1193–1194.

[18] T. Sugihara and Y. Nakamura, "Whole-body Cooperative COG Control through ZMP Mnipulation for Humanoid Robots," in *IEEE Int. Conf. on Robotics and Automation*, Washington DC, USA, 2002.

[19] S. Kajita, F. Kanehiro, K. Kaneko, K. Fujiwara, K. Yokoi, and H. Hirukawa, "Biped walking pattern generation by a simple three-dimensional inverted pendulum model," *Advanced Robotics*, vol. 17, no. 2, pp. 131–147, 2004.

[20] G. Cheng, S. Hyon, J. Morimoto, A. Ude, J. G. Hale, G. Colvin, W. Scroggin, and S. C. Jacobsen, "CB: a humanoid research platform for exploring neuroscience," *Advanced Robotics*, vol. 21, no. 10, pp. 1097–1114, 2007.

[21] S. H. Strogatz, *Nonlinear Dynamics and Chaos*. Addison-Wesley Publishing Company, 1994.

[22] N. Yamasaki, M. Kawachi, T. Nishizawa, T. Suzuki, and A. Kusumoto, *Encyclopedia of foot (in Japanese)*. Asakura Shoten, 1999.

[23] J. Perry, *Gait Analysis: Normal and Pathological Function*. Slack Inc., 1992.

[24] D. A. Winter, *Biomechaniics and Motor Control of Human Movement*, Second ed. John Wiley & Sons, Inc., 1990.

[25] J. Morimoto and C. G. Atkeson, "Minimax differential dynamic programming: An application to robust biped walking," in *Advances in Neural Information Processing Systems 15*, S. Becker, S. Thrun, and K. Obermayer, Eds. Cambridge, MA: MIT Press, 2003, pp. 1563–1570.

[26] J. Morimoto and C. G. Atkeson, "Learning Biped Locomotion: Application of Poincaré-Map-Based Reinfrocement Learning," *IEEE Robotics and Automation Magazine*, vol. 14, no. 2, pp. 41–51, 2007.